Buck-Type Current Unfolding Converter With Discontinuous Conduction Mode in Ultra-Low Power-Factor Operation

Tomoyuki Mannen [1], Boseung Seo[1], Takanori Isobe[1], Ha Pham N.[2]

[1] University of Tsukuba, Japan
[2] University of Technology, Sydney, Australia

Corresponding author: Tomoyuki Mannen, mannen@ieee.org
Speaker: Tomoyuki Mannen, mannen@ieee.org

Abstract

This paper proposes a control method for a buck-type current unfolding converter, especially operating under non-unity power factor. The proposed method utilizes discontinuous conduction mode (DCM) to control the inductor current. DCM enables the converter to drastically reduce its inductors and allows the current controller to handle step changes in current due to non-unity power factor operations. Furthermore, this method enables the application of a feedforward-based control strategy by utilizing DCM, thereby eliminating the need for current sensors in the converter. Experimental results demonstrate sinusoidal output current waveforms at both unity and zero power factors, achieved without any current sensors in the converter prototype. These results confirm the effectiveness of the proposed method, particularly its robust current control capabilities. The proposed method is expected to increase the switching frequency and reduce the size of the passive components.

1 Introduction

Growing demand for renewable energy accelerates the requirement for improved efficiency and miniaturization of power converters, leading to a wide variety of research efforts. Utilizing new power device structures and wide-band-gap semiconductors can enhance converter performance due to their fast switching and low on-resistance, effectively reducing losses and allowing for smaller cooling components and passive elements [1, 2].
Moreover, various circuit topologies, such as multilevel topologies, neutral-point-clamped (NPC) converters, and T-type configurations, have attracted attention for their ability to achieve higher efficiency and smaller sizes [3–5]. Discontinuous PWM, which is a well known-method, reduces the number of switching to 2/3 by using common-mode voltage in the three-phase converter. Reference [6] has proposed one-phase PWM for three-phase converters which can reduces the number of the switching to 1/3 and improve its efficiency.
Current unfolding converters separate a current control unit and a current unfolding unit, enabling them to reduce the number of switches operating with high-frequency PWM. As a result, the current unfolding converters can reduce the total number of switching and inductors compared to conventional three-phase converters [7, 8]. However, it may be difficult for the current unfolding converters to regulate the output currents during leading or lagging power factor operations due to sudden current changes [9]. This is because popular converters, includes the current unfolding converters, operate in continuous conduction mode (CCM), leading to delayed and restricted response from the current controller.
In contrast, the discontinuous conduction mode (DCM) offers faster current control, zero current switching, and increased stability by implementing feedforward-based control without accumulating control errors [10]. The DCM can increase the switching frequency and contribute to reducing the size of the inductor [11, 12].
This paper proposes a control method utilizing DCM for the current unfolding converter in order to enable ultra-low power factor operation. The current control using the DCM makes it possible to follow step change references caused by the non-unity power factor operations. Since the proposed control method is based on feedforward control, the current unfolding converter can eliminate current sensors for its feedback control and instability

problem due to control delay. Experimental verification using a prototype of the current unfolding converter clarifies a good current control capability of the proposed method. The experimental results exhibit sinusoidal current waveforms at both unity and zero power factor, even though there is no current sensor in the converter. The proposed method is useful for increasing the switching frequency and reducing passive components.

2 Circuit Configuration and Operating Principle

Fig. 1 shows the circuit diagram of a buck configuration for a current unfolding converter. This converter is divided into two units: a current regulation unit and a current unfolding unit. The current regulation unit consists of four switches and two inductors, upper and lower choppers, which are connected in a vertically symmetrical manner. This unit operates with high-frequency PWM, and the two choppers regulate two intermediate currents, i_+ and i_-. Since the sum of the three-phase currents should be zero, the remaining intermediate current i_0 is regulated without further modulation once i_+ and i_- have been determined. Therefore, the current regulation unit forms the intermediate currents i_+, i_0, and i_- as part of the three-phase currents.

The current unfolding unit consists of a three-phase T-type NPC converter configuration. However, this unit operates at the line frequency, and unfolds and rearranges the three intermediate currents i_+, i_0, and i_-. Fig. 2 shows the switching patterns of the current unfolding unit. The operation of the current unfolding unit depends on the magnitude order of the phase voltages of the ac source.

The phase with the highest voltage is connected to the upper-side intermediate terminal through one of the upper-side switches, $S_{\mathrm{u}+}$, $S_{\mathrm{v}+}$, or $S_{\mathrm{w}+}$. Similarly, the phase with the lowest voltage is connected to the lower-side intermediate terminal through one of the lower side switches, $S_{\mathrm{u}-}$, $S_{\mathrm{v}-}$, or $S_{\mathrm{w}-}$. The other phase, with the middle voltage, connects to the common terminal through one of the common-side bidirectional switches, $S_{\mathrm{u}0}$, $S_{\mathrm{v}0}$, or $S_{\mathrm{v}0}$. When the output of the converter is connected to a balanced three-phase ac line, each switching device operates at the line frequency or twice the line frequency. The rearranged currents form the three-phase ac currents i_{u}, i_{v}, and i_{w}.

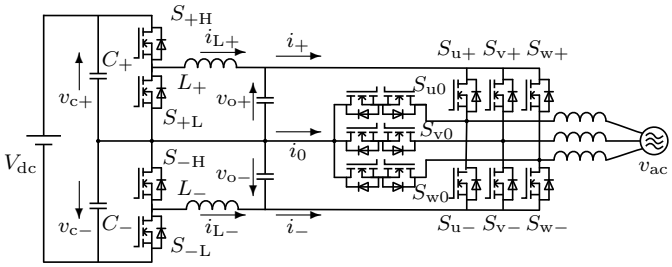

Fig. 1: A circuit diagram of the current unfolding converter.

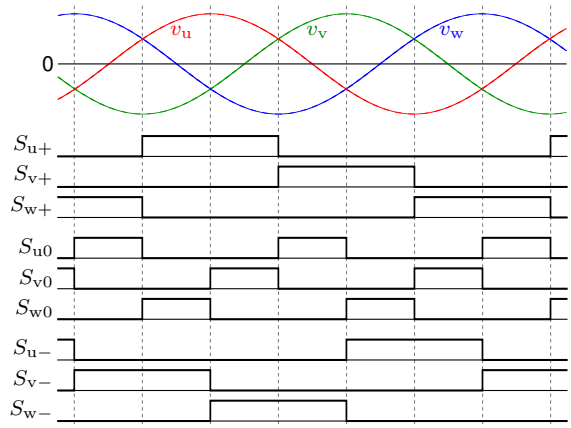

Fig. 2: Operating principles of the current unfolding unit.

3 Non-unity Power Factor Operation

Fig. 3 shows schematic waveforms of the current unfolding converters. Fig. 3a represents the operation under the unity power factor condition. Each intermediate current exhibits a continuous waveform because the crossing point of the output current coincides with the commutation timing of the current unfolding unit.

On the other hand, Fig. 3b shows the waveforms of non-unity power factor operation. The output current is shifted according to the power factor, and the intermediate current waveforms exhibit jumps at the point of commutation in the unfolding unit. In this case, the current unfolding unit swaps two current paths that have different amplitudes, due to the phase difference between the voltage and current.

3.1 Operating with Continuous Conduction Mode (CCM)

Since the inductor current in CCM requires feedback for current control, the current regulation unit employs proportional control with a feedback gain K_{C}. Additionally, integral or resonant control may

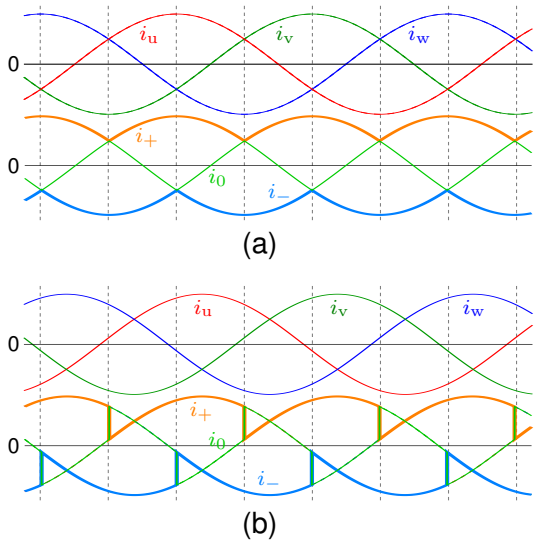

Fig. 3: A schematic waveforms of intermediate currents in (a) the unity power factor and (b) the low power factor.

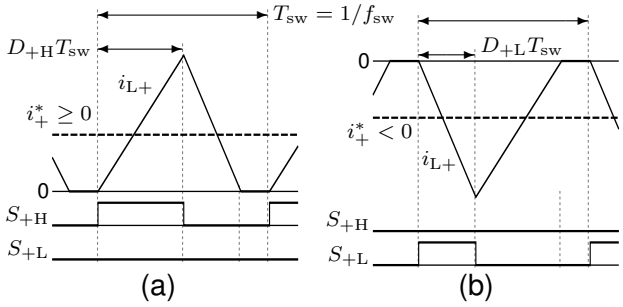

Fig. 4: Operation principles of current control in DCM when (a) $i_+^* \geq 0$ and (b) $i_+^* < 0$.

sometimes enhance the feedback characteristics in steady states. In non-unity power factor operation, the current controller must be able to track step changes in the current waveforms. Increasing the feedback gain extends the control bandwidth; however, it can also induce stability problems. A higher switching frequency and/or a smaller ac inductor have the potential to achieve a wider control bandwidth. Nevertheless, the actual system cannot reduce the control delay, which is due to the sensors used for feedback and the calculations in DSPs. Since control delay is the most critical factor inducing instability in the feedback control, the current control bandwidth is limited, making it impossible for CCM operation to exceed these limits.

3.2 Operating with Discontinuous Conduction Mode (DCM)

The current regulation unit operating in discontinuous conduction mode (DCM) may improve current control performance because DCM does not require feedback control and can operate using feedforward-based control. Fig. 4 shows the operation principles of the current regulation unit with DCM. When the operating power factor is close to unity, the upper- and lower-side chopper operate in uni-direction, with $i_{L+} > 0$ and $i_{L-} > 0$, due to the operation in the current unfolding unit. Conversely, when the output power factor is low, both the upper- and lower-side choppers require bi-directional operation in the fundamental cycle of ac mains.

Focusing on the upper-side chopper, which regulates the upper-side intermediate current i_+, when the direction of the intermediate current is $i_+ > 0$, only the switch S_{+H} operates with PWM and the other one S_{+L} remains turned off. Assuming that the average of the upper-side inductor current i_{L+} corresponds to the intermediate current i_+, the duty ratio of the switch S_{+H} is given by

$$D_{+H} = \sqrt{\frac{2f_{sw}L_+I_{L+}v_{o+}}{v_{c+}(v_{c+} - v_{o+})}} \tag{1}$$

where v_{o+} is the output voltage of the chopper and v_{c+} is the voltage of the upper-side capacitor C_+, which serves as the input voltage of the chopper, and f_{sw} is the switching frequency of the chopper. On the other hand, when the intermediate current has the opposite direction, $i_+ < 0$, only the switch S_{+L} operates with PWM, and S_{+H} remains turned off. Similarly, the duty ratio for S_{+L} is given by

$$D_{+L} = \sqrt{\frac{2f_{sw}L_+I_{L+}(v_{o+} - v_{c+})}{v_{o+}v_{c+}}}. \tag{2}$$

In the same manner, the lower-side chopper regulates the lower-side intermediate current i_-. The direction of i_- also determines which switch operates with PWM: S_{-H} when $i_- > 0$ and S_{-L} when $i_- > 0$. Its duty ratios D_{-H} and D_{-L} are also calculated by

$$D_{-H} = \sqrt{\frac{2f_{sw}L_-I_{L-}(v_{o-} - v_{c-})}{v_{o-}v_{c-}}}, \tag{3}$$

$$D_{-L} = \sqrt{\frac{2f_{sw}L_-I_{L-}v_{o-}}{v_{c-}(v_{c-} - v_{o-})}} \tag{4}$$

where v_{o-} is the output voltage of the chopper and v_{c-} is the voltage of the lower-side capacitor C_-. Here, the phase difference between the output current and ac line voltage is defined as ϕ. When $|\phi| \geq \pi/6$, the choppers switch the operating mode with PWM according to the phase angle.

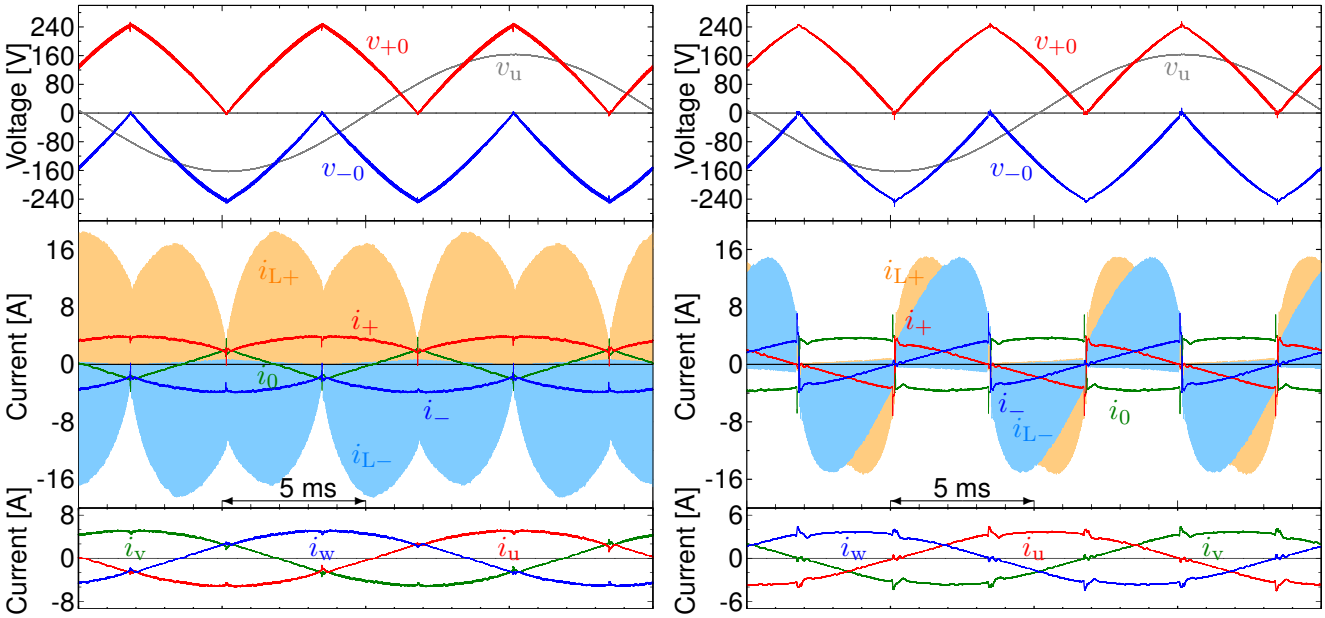

Fig. 5: Experimental waveforms of the proposed current unfolding converter operating under (a) unity power factor $\cos\phi = 1$ and (b) ultra-low power factor $\cos\phi = 0$.

Tab. 1: Circuit parameters used for experiments

DC source voltage	$V_{\rm dc}$	550 V
AC line-to-line voltage	$V_{\rm ac}$	200 V
AC Line frequency	$f_{\rm ac}$	50 Hz
Switching frequency	$f_{\rm sw}$	50 kHz
DCM inductor	L_+, L_-	30 μH
Filter capacitor	$C_{\rm f}$	4.7 μF
AC Filter inductor	$L_{\rm ac}$	150 μH

4 Experimental Results

Fig. 5 shows experimental waveforms of the proposed current unfolding converter operating with DCM. A fabricated prototype of the proposed converter employs SiC-MOSFETs for both the current regulation unit and the current unfolding unit. Since the switching frequency of the current regulation unit was fixed at $f_{\rm sw} = 50$ kHz, the switching inductors and the filter capacitors for DCM were designed as $L_+ = L_- = 30$ μH and $C_{\rm f} = 4.7$ μF, respectively. The prototype was connected with a dc voltage source, whose set voltage was $V_{\rm dc} = 550$ V, on its high-voltage side of the current regulation unit though series-connected dc capacitors. The ac-side of the prototype was also connected to a three-phase ac voltage source through an additional three-phase filter inductor. The set voltage of the ac source was $V_{\rm ac} = 200$ V and its frequency was $f_{\rm ac} = 50$ Hz. In the following experiments, the ac current reference was set to $I^*_{\rm ac} = 2.8$ A, resulting in an output of 1 kVA.

Fig. 5a shows measured waveforms operating under a unity power factor $\cos\phi = 1$. The intermediate voltages $v_{\rm o+}$ and $v_{\rm o-}$ followed the difference between the highest and middle ac voltages $v_+ - v_0$ and the lowest and middle ac voltages $v_- - v_0$, respectively. The inductor currents $i_{\rm L+}$ and $i_{\rm L-}$ included large current ripples due to DCM operation; however, the intermediate currents i_+, i_0, and i_- were well regulated as rearranged three-phase sinusoidal currents. As a result, the ac currents $i_{\rm u}$, $i_{\rm v}$, and $i_{\rm w}$ had a sinusoidal current shape. In unity power factor operation, the peak of inductor current was 18 A which is 4.5 times higher than the ac current.

Fig. 5b is the waveforms when the converter operates under a power factor $\cos\phi = 0$. Its voltage waveforms were the same shape as those in Fig. 5a. On the other hand, both inductor currents $i_{\rm L+}$ and $i_{\rm L-}$ exhibited bidirectional output due to ultra-low power factor operation. Even though the intermediate currents i_+, i_0, and i_- included step changes when the intermediate voltage $v_{\rm o+}$ or $v_{\rm o-}$ became to zero, the currents followed the step changes well. The ac output currents were sometimes distorted around $v_{\rm o+} = 0$ or $v_{\rm o-} = 0$, but the

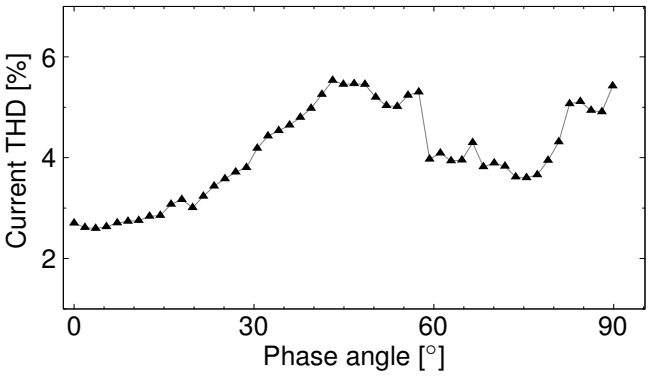

Fig. 6: Measured current THDs of the proposed current unfolding converter in various operating power factor.

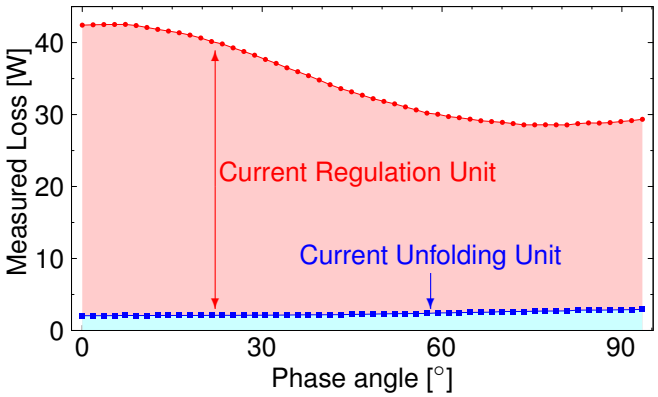

Fig. 7: Measured loss of the proposed current unfolding converter in various operating power factor.

current waveforms maintained a sinusoidal shape. Therefore, the DCM enables the proposed converter possible to operate under ultra-low power factor conditions, even though the current reference includes step changes.

Fig. 6 shows measured total harmonic distortion (THD) of the ac current in the proposed converter under various operating power factors. The current phase angle ϕ was shifted from 0 to $\pi/2$. When the operating point was close to the unity power factor, the THD reached a minimum value of 2.6%. On the other hand, the maximum THD was 5.4% around $\phi = 45°$ and $90°$ due to large steps in the intermediate currents.

Fig. 7 shows measured conversion losses of the proposed converter across various operating power factors. The loss in the current unfolding unit slightly increased with the increase of phase angle ϕ, however, the loss was less than 10% of the total loss. Since the current unfolding unit operates at the ac-line frequency or double line frequency, there is almost no switching loss and the dominant loss is due to conduction. Conversely, since the current regulation unit operates with high-frequency PWM at 50 kHz, the predominant losses of the proposed converter occur in this unit. As the peak of the inductor current decreased with the increase of phase angle ϕ, the loss in the current regulation unit also decreased.

5 Conclusion

This paper proposed a control method utilizing DCM for the buck-type current unfolding converter. The DCM operation enables the current regulator of the unfolding converter to follow step change references required by non-unity power factor operations. In ultra-low power factor operations, where $|\phi| \geq \pi/6$, the proposed control method selects two of the four switches operating at the high-frequency PWM in the current regulation unit based on the current direction. Since the proposed control method is based on feedforward control, it allows the current unfolding converter to eliminate the need for current sensors for its feedback control, thus freeing it from instability problems associated with higher switching frequencies and/or faster current regulation.

This paper verified the validity of the proposed method through experiments using a prototype of the current unfolding converter. The experimental results demonstrated that the DCM operation successfully followed step changes in the intermediate currents. As a result, the ac current THD of the proposed method achieved 2.6% at the unity power factor and 5.4% at the low power factor, even though the converter operated solely with feedforward control and without current sensors.

The proposed method is useful for increasing the switching frequency and reducing passive components.

References

[1] J.W. Kolar, D. Neumayr, D. Bortis, “Google Little Box Reloaded: How to Achieve 200W/in^3 & Beyond? Concepts - Evaluation - Barriers - Future,” *IEEE APEC 2017*, 2017.

[2] A. Hariya, T. Koga, K. Matsuura, H. Yanagi, S. Tomioka, Y. Ishizuka, T. Ninomiya, “Circuit Design Techniques for Reducing the Effects of Magnetic Flux on GaN-HEMTs in 5-MHz 100-W High Power-Density LLC Resonant DC–DC Converters,” *IEEE Transactions*

on Power Electronics, vol. 32, no. 8, pp. 5953-5963, 2017.

[3] D. M. Baker, V. G. Agelidis and J. Y. Chen, "A five-level zero average current error controlled single-phase grid-interactive inverter," *International Conference on Power Electronic Drives and Energy Systems for Industrial Growth*, vol. 1, no. 6, pp. 50–55, 1998.

[4] L. B. G. Campanhol, S. A. O. da Silva, A. A. de Oliveira and V. D. Bacon, "Dynamic Performance Improvement of a Grid-Tied PV System Using a Feed-Forward Control Loop Acting on the NPC Inverter Currents," *IEEE Transactions on Industrial Electronics*, vol. 64, no. 3, pp. 2092–2101, 2017.

[5] A. Anthon, Z. Zhang, M. A. E. Andersen, D. G. Holmes, B. McGrath and C. A. Teixeira, "The Benefits of SiC mosfets in a T-Type Inverter for Grid-Tie Applications," *IEEE Transactions on Power Electronics*, vol. 32, no. 4, pp. 2808–2821, 2017.

[6] E. Serban, F. Paz and M. Ordonez, "Improved PV Inverter Operating Range Using a Miniboost," *IEEE Transactions on Power Electronics*, vol. 32, no. 11, pp. 8470–8485, 2017.

[7] T. B. Soeiro, T. Friedli and J. W. Kolar, "Swiss rectifier – A novel three-phase buck-type PFC topology for Electric Vehicle battery charging," 2012 Twenty-Seventh Annual IEEE Applied Power Electronics Conference and Exposition (APEC), pp. 2617–2624, 2012.

[8] B. Seo, T. Mannen and T. Isobe, "Suppression Method of DC Capacitor Currents in a Three-Phase Current Unfolding Inverter Equipped With Ultra-Small DC Capacitors," *2022 IEEE 31st International Symposium on Industrial Electronics (ISIE).*, pp. 939–942, 2022.

[9] T. Mannen, P. N. Ha and K. Wada, "Performance Evaluation of a Boost Integrated Three-Phase PV Inverter Operating With Current Unfolding Principle," *2019 21st European Conference on Power Electronics and Applications (EPE'19 ECCE Europe).*, pp. 1–8, 2019.

[10] D. Murillo-Yarce, C. Restrepo, D. G. Lamar and J. Sebasti´an, "A General Method to Study Multiple Discontinuous Conduction Modes in DC-DC Converters With One Transistor and Its Application to the Versatile Buck-Boost Converter," *IEEE Transactions on Power Electronics*, vol. 37, no. 11, pp. 13030–13046, 2022.

[11] J. Roy, A. Gupta and R. Ayyanar, "Discontinuous Conduction Mode Analysis of High Gain Extended-Duty-Ratio Boost Converter," *IEEE Open Journal of the Industrial Electronics Society*, vol. 2, pp. 372–387, 2021.

[12] V. Leonavicius, M. Duffy, U. Boeke and S. C. O. Mathuna, "Comparison of realization techniques for PFC inductor operating in discontinuous conduction mode," *IEEE Transactions on Power Electronics*, vol. 19, no. 2, pp. 531–541, 2004.